Further Perspectives on the Teflate vs. Fluoride Analogy: The Case of a Co(II) Pentafluoroorthotellurate Complex

Alberto Pérez-Bitrián,[a] Julen Munárriz,[b] Johanna S. Sturm,[a] Daniel Wegener,[a] Konstantin B. Krause,[c] Anja Wiesner,[a] Christian Limberg,[c] Sebastian Riedel*[a]*

[a] Fachbereich Biologie, Chemie, Pharmazie, Institut für Chemie und Biochemie – Anorganische Chemie, Freie Universität Berlin, Fabeckstraße 34/36, 14195 Berlin (Germany).

[b] Departamento de Química Física y Analítica, Universidad de Oviedo, Julián Clavería n° 8, Campus Universitario de El Cristo, 33006 Oviedo (Spain).

[c] Institut für Chemie, Humboldt-Universität zu Berlin, Brook-Taylor-Straße 2, 12489 Berlin (Germany).

Keywords

Pentafluoroorthotellurate, cobalt, electronic structure, coordination chemistry, fluorine chemistry, theoretical chemistry, chemical bond

Abstract

The pentafluoroorthotellurate group (teflate, $OTeF_5$) is considered as a bulky analogue of fluoride, yet its coordination behavior in transition-metal complexes is not fully understood. By reaction of $[CoCl_4]^{2-}$ and neat $ClOTeF_5$, we have synthesized the first cobalt teflate complex, $[Co(OTeF_5)_4]^{2-}$, which exhibits moisture-resistant Co–$OTeF_5$ bonds. Through a combined experimental and theoretical (DFT and NEVPT2) study, the properties and electronic structure of this species have been investigated. It exhibits a distorted tetrahedral structure around the cobalt center and can be described as a d^7 system with a quartet (S = 3/2) ground state. A comparative bonding analysis of the (pseudo)tetrahedral $[CoX_4]^{2-}$ anions (X = $OTeF_5$, F, Cl) revealed that the strength of the Co–X interaction is similar in the three cases, being the strongest in $[Co(OTeF_5)_4]^{2-}$. In addition, an analysis of the charge of the Co center reinforced the similar electron-withdrawing properties of the teflate and the fluoride ligands. Therefore, the $[Co(OTeF_5)_4]^{2-}$ anion constitutes an analogue of the polymeric $[CoF_4]^{2-}$ in terms of electronic properties, but with a monomeric structure.

1. Introduction

The pentafluoroorthotellurate group (teflate, $OTeF_5$) is a unique ligand, which often forms the only stable analogues of the corresponding metal fluorides.[1,2] This is due to the similar electron-

withdrawing character of the fluoride and the teflate ligand, which is accompanied in the case of the teflate by a much higher steric demand. Additionally, its high charge delocalization makes it very robust against electrophiles, enabling the preparation of different weakly coordinating anions,[3] as well as the stabilization of high-oxidation-state complexes and highly reactive species.[1,2] Interestingly, unlike the fluorides, metal teflates usually show molecular structures due to the low tendency of this ligand to form bridges. Despite the number of teflate compounds prepared thus far, the coordination chemistry of transition-metal teflate complexes has remained far less developed than that of main-group elements. In fact, it has only recently been demonstrated that the teflate group also behaves as a weak/medium-field ligand, similarly to the fluoride,[4] and can also lead to transition-metal-based Lewis superacids.[5]

Homoleptic transition-metal complexes are prototypical species in the development of coordination and organometallic chemistry due to their simple nature.[6–8] In the particular case of first-row transition-metal teflate complexes, only few representatives are known, which has hindered the understanding of some fundamental physical and chemical properties associated to the teflate ligand. These examples are limited to the neutral $[Ti(OTeF_5)_4]$ and the anionic $[Ti(OTeF_5)_6]^{2-}$ species,[9–11] as well as the neutral $[Fe(OTeF_5)_3]$, structurally characterized as the $[Fe(OTeF_5)_3{\cdot}3SO_2ClF]$ adduct.[12] Our recent investigation of the homoleptic $[Ni(OTeF_5)_4]^{2-}$ anion[4] prompted us to extend our study to other 3*d* transition-metal teflate complexes with the aim to better understand the coordination chemistry of this ligand. The key role of cobalt in the development of coordination chemistry[13] captured our attention to this metal, for which, additionally, no teflate complex had been reported so far. Nevertheless, in 1991 a very insoluble compound whose composition should correspond to $[Co(OTeF_5)_3]$ was claimed to be prepared by reaction of $CoCl_2$ and $ClOTeF_5$, but no characterization was provided.[12] Additionally, the

homoleptic $[Co(OTeF_5)_4]^{2-}$ anion was alluded to in a review in 1993, but its synthesis, characterization or properties have never been reported.[14]

Within this context, we now present a combined experimental and theoretical study on the first compound containing Co–$OTeF_5$ bonds, $[NEt_4]_2[Co(OTeF_5)_4]$. Different structural and electronic properties are investigated and a bond analysis is performed, with the aim of shedding light on the teflate/fluoride analogy in coordination chemistry.

2. Results and discussion

2.1. Synthesis and characterization of $[NEt_4]_2[Co(OTeF_5)_4]$

The $[NEt_4]_2[CoCl_4]$ salt reacts with neat $ClOTeF_5$ to produce $[NEt_4]_2[Co(OTeF_5)_4]$ selectively as a bright blue powder in quantitative yield (Scheme 1). As a side-product, Cl_2 is formed, which is removed from the reaction mixture by evaporation. This preparative approach is similar to that used for the synthesis of the related Ni[4] or Au[5] homoleptic anions, therefore entailing yet another example for the practicability of using the hypochlorite $ClOTeF_5$[15,16] in the synthesis of teflate compounds.[12,17–21]

$$[NEt_4]_2[CoCl_4] + 4\ ClOTeF_5 \xrightarrow[-\ 4\ Cl_2]{} [NEt_4]_2[Co(OTeF_5)_4]$$

Scheme 1. Synthesis of $[NEt_4]_2[Co(OTeF_5)_4]$.

The molecular structure of $[NEt_4]_2[Co(OTeF_5)_4]$ in the solid state was determined by single-crystal X-ray diffraction (see Supporting Information for details). The cations and the anion appear well-separated, much like in the complex $[PPh_4]_2[Co(OPh)_4]$.[22] This is contrary to the case of the related $[Co(OR)_4]^{2-}$ anions (R = C_6F_5, 3,5-$C_6H_3(CF_3)_2$, C_4F_9),[23–26] in which strong interactions of the O atoms with the metal cations further deform the geometries around the

metal center. The {CoO_4} core of the $[Co(OTeF_5)_4]^{2-}$ anion (Figure 1) can be described as a distorted tetrahedron. The distortion can be easily inferred already from the O–Co–O angles (94.9(3)–120.9(3)°), which lead to a calculated geometry index[27] of $\tau_4 = 0.88$, indicating a rather prominent deformation from the regular tetrahedron ($\tau_4 = 1.00$). This entails a symmetry close to D_{2d} for the {$Co^{II}O_4$} entity, which results in an overall approximate S_4 molecular symmetry when considering the special arrangement of teflate ligands.

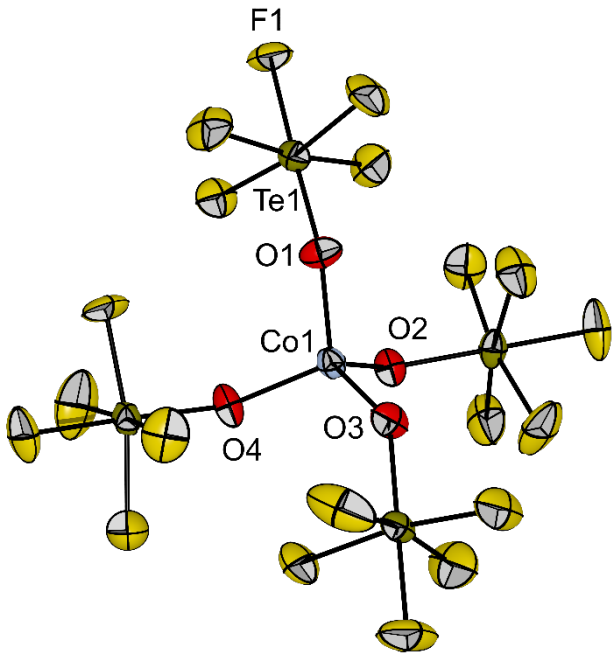

Figure 1. Molecular structure of the $[Co(OTeF_5)_4]^{2-}$ anion in the solid state as found in crystals of $[NEt_4]_2[Co(OTeF_5)_4]$. The $[NEt_4]^+$ cations have been omitted for clarity. Displacement ellipsoids set at 50% probability. Only one set of the disordered F atoms found in the $[OTeF_5]^-$ ligand containing O4 is shown. Selected bond lengths [pm] and angles [°]: Co–O1 194.9(7), Co–O2 195.7(7), Co–O3 193.3(7), Co–O4 195.3(6), O1–Co–O2 115.6(3), O1–Co–O3 100.1(3), O1–Co–O4 113.5(3), O2–Co–O3 112.8(3), O2–Co–O4 94.9(3), O3–Co–O4 120.9(3). For crystallographic details see Supporting Information.

The distorted tetrahedral structure of the $[Co(OTeF_5)_4]^{2-}$ anion already suggests a spin configuration with three unpaired electrons (S = 3/2).[6] An effective magnetic moment of μ_{eff} = 5.03 μ_B was measured for $[NEt_4]_2[Co(OTeF_5)_4]$, which was found to be temperature-independent. This value is significantly higher than the spin-only value of μ_{eff} = 3.87 μ_B, corresponding to three unpaired electrons. This is due to orbital contributions to the magnetic moment, derived from the orbital mixing (spin-orbit coupling constant λ = –170 cm^{-1} for Co^{2+}), which are neglected in the spin-only formula.[28,29] Nevertheless, this value is in agreement with other reported effective magnetic moments of high-spin Co(II) complexes with formulas $[CoX_4]^{2-}$ (X = anionic ligand), which range between 4.4 and 5.1 μ_B.[24,25,26,30,31] Therefore, the $[Co(OTeF_5)_4]^{2-}$ anion can be described as a d^7 system with a quartet (S = 3/2) ground state. Additionally, a simulation of the magnetic data was successfully performed, as shown in Figure 2. All fit parameters for $[NEt_4]_2[Co(OTeF_5)_4]$ are reported in the Supporting Information.

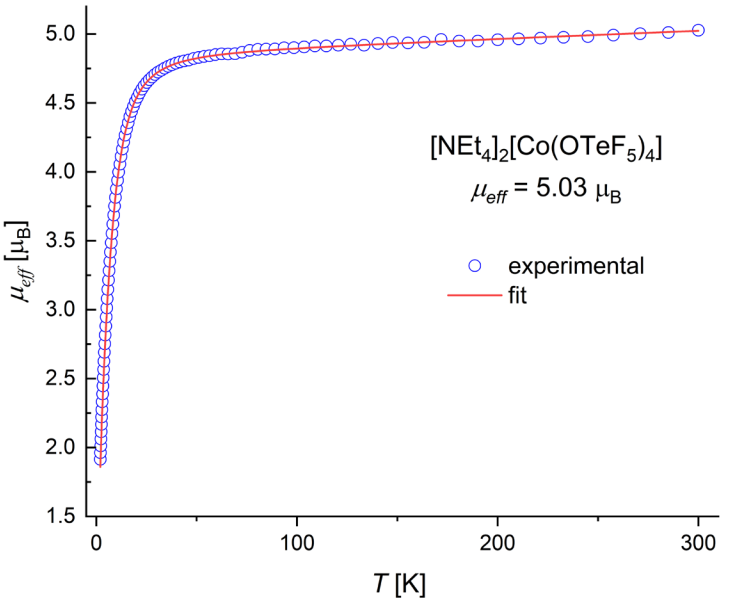

Figure 2. Experimental μ_{eff} versus T plot and fit for compound $[NEt_4]_2[Co(OTeF_5)_4]$.

2.2. Electronic configuration of the $[Co(OTeF_5)_4]^{2-}$ anion

To attain a better understanding of the electronic properties of the $[Co(OTeF_5)_4]^{2-}$ anion, we performed a series of theoretical calculations. We found that the structure optimization of the quartet ground state at the B3LYP-D3BJ/def2-TZVP and M06L/def2-TZVP levels of theory renders structures that are in good agreement with the experimental one and, in fact, the distortion at the Co center persists (see Computational details). The range of O–Co–O angles (99.6–114.7° and 98.0–116.3°, respectively) is slightly narrowed with respect to the experimental values, but leads to very similar geometry indexes (τ_4 = 0.93 and τ_4 = 0.91, for BLYP and M06L, respectively).

Despite the good agreement between the experimental and the DFT-optimized structures, we performed multireference calculations to unravel potential multiconfigurational effects that might make single-reference DFT calculations unsuitable for the study of the electronic structure of the system. In particular, we analyzed the electronic structure of the $[Co(OTeF_5)_4]^{2-}$ anion by combining state-average complete active space self-consistent field (SA-CASSCF),[32] with the perturbative treatment of dynamic electron correlation provided by *n*-electron valence state perturbation theory (NEVPT2).[33–35] In the SA-CASSCF calculation, we considered 10 quartet and 10 doublet states. In a hypothetically perfect tetrahedral geometry, they would correspond to the following terms: $^4A_2$, $^4T_2$, $^4T_1(F)$, $^4T_1(P)$, $^2E_2$, $^2T_1$, $^2T_2$, $^2A_1$ and $^2A_2$. In the active space, we included the molecular orbitals mainly composed by the metal 3*d* orbitals as well as the Co–O orbitals with significant 3*d* contribution. Additionally, to account for the well-known double-*d* shell correlation effects, we also included in the calculation the 4*d* orbitals of Co.[36–38] The active space molecular orbitals are provided in Figure S5 and the energies and composition for the different states are provided in Table S4. At this point, the most relevant information is related to

the ground state of the $[Co(OTeF_5)_4]^{2-}$ anion, which, as expected, corresponds to the pseudo-$^4A_2$ quartet state (in tetrahedral notation). Such state can be considered to be mainly single reference, with the $3d_{z^2}{}^2 3d_{x^2-y^2}{}^2 3d_{xy}{}^1 3d_{yz}{}^1 3d_{xz}{}^1$ electronic configuration (Figure 3) accounting for 97.9% of the CAS wave function. The fact that the ground state of our system is mainly single reference justifies, in broad strokes, the use of DFT for describing it, considering in addition (i) that the electronic configuration according to the multireference calculations corresponds to the DFT-computed ground state, which in turn, is in line with the three unpaired electrons derived from the determined effective magnetic moment of $[NEt_4]_2[Co(OTeF_5)_4]$ (*vide supra*), and (ii) that the experimental (Figure 1) and the computed structures are in very good agreement. Regarding the electronic structure, the calculations further revealed that the first doublet state is 219 kJ mol^{-1} higher in energy, providing additional evidence for the quantitative population of the quartet ground state. As commented above, although the deviation from the tetrahedral structure in the $\{CoO_4\}$ local environment is not very pronounced, the spatial distribution of the teflate ligands results in a molecular symmetry that is very close to S_4. This leads to a further splitting of the orbitals, as schematically shown in Figure 3.

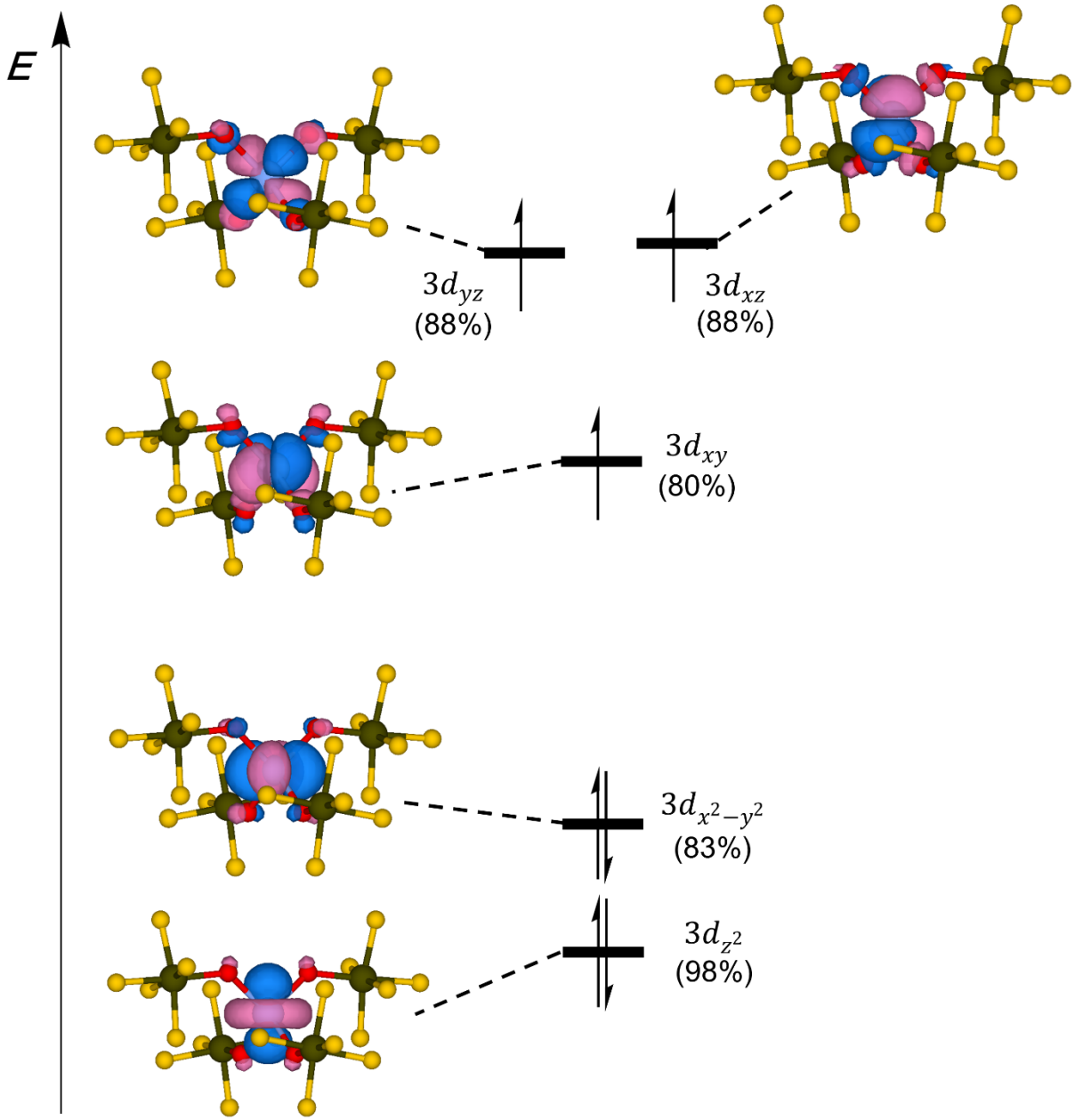

Figure 3. Schematic representation of the energy diagram of the MOs mainly composed by Co 3*d* orbitals. MOs correspond to the SA-CASSCF(15,14) ones, and the highest Löwdin orbital composition is shown in parenthesis.

We now proceed to analyze in detail the coordination effects of the teflate ligand. The obvious compound to compare with would be the corresponding fluoride analogue. Unfortunately, the

extended layered structure of $[CoF_4]^{2-}$, containing corner-sharing $\{CoF_6\}$ octahedra,[39–42] prevents comparing the effect on a (pseudo)tetrahedral coordination environment. In this context, the prototypical $[CoCl_4]^{2-}$ anion seemed like a good candidate for such analysis. For the sake of comparison, we will focus on the $[NMe_4]^+$ salt, which should provide a similar chemical environment, with well-separated cations and anions. The fact that the Cl–Co–Cl angles vary here from 108.3(2)° to 112.8(4)°, leading to a slight distortion towards D_{2d} symmetry (τ_4 = 0.97),[43] has been rationalized – via comparison with the related $[NiCl_4]^{2-}$ and $[ZnCl_4]^{2-}$ complex anions – by crystal packing forces.[43] This interpretation is in line with the finding that optimization of the $[CoCl_4]^{2-}$ anion (B3LYP-D3BJ/def2-TZVP level of theory) leads to a perfectly tetrahedral coordination sphere. In fact, when the structure of a hypothetically discrete $[CoF_4]^{2-}$ anion is optimized, it also has T_d symmetry in the ground state.

Due to the simplicity of the $[Co(OTeF_5)_4]^{2-}$ anion, electronic spectroscopy can help to get insights into its electronic structure. The description will be done in terms of a hypothetical tetrahedral ligand field, which is the one that has been used to perform such studies with the well-investigated $[CoCl_4]^{2-}$ anion, as well as with the related $[Ni(OTeF_5)_4]^{2-}$ compound.[4] Tetrahedral $[CoX_4]^{2-}$ species exhibit a $^4A_2$ ground term and three transitions are observed in their UV-Vis spectra: ν_1 ($^4T_2 \leftarrow {}^4A_2$), ν_2 ($^4T_1(F) \leftarrow {}^4A_2$), and ν_3 ($^4T_1(P) \leftarrow {}^4A_2$).[31,44] The spectrum of compound $[NEt_4]_2[Co(OTeF_5)_4]$ (Figure 4) is qualitatively the same as for other tetrahedral $[CoX_4]^{2-}$ species, including both the thoroughly investigated tetrahalogenidocobaltates (X = Cl, Br, I),[30] as well as other homoleptic compounds in which X is an O-donor ligand.[23–25] As expected, we observe mainly the ν_3 absorption, split into several components as in case of the tetrachloridocobaltate(II) anion, for which spin-orbit coupling in combination with dynamic Jahn-Teller effects in the excited states were discussed as the origins.[30] In the case of

$[Co(OTeF_5)_4]^{2-}$ also a symmetry lowering could be responsible. Transition ν_1 lies at low energy and therefore cannot be observed in our measurement window, similarly to ν_2, which cannot be observed entirely. Overall, these d–d transitions appear blue-shifted with respect to those of the $[CoX_4]^{2-}$ complexes (X = Cl, Br, I), suggesting an increase in the ligand-field strength in the order $I^- < Br^- < Cl^- < [OTeF_5]^-$. This highlights the fact that the teflate group is an analogue of fluoride in ligand-field terms.[4] At this point, we note that the UV-Vis spectrum is in agreement with our NEVPT2 calculations. Namely, the ν_3 transition is predicted to lie in the range of 19237–19356 cm^{-1}, and ν_2 in the range of 6447–6822 cm^{-1}. While the deviation is significant for ν_3, we consider the spectra description to be qualitatively correct, especially taking into account that relativistic and environment effects were not considered and that no approximation to the basis set limit was made.

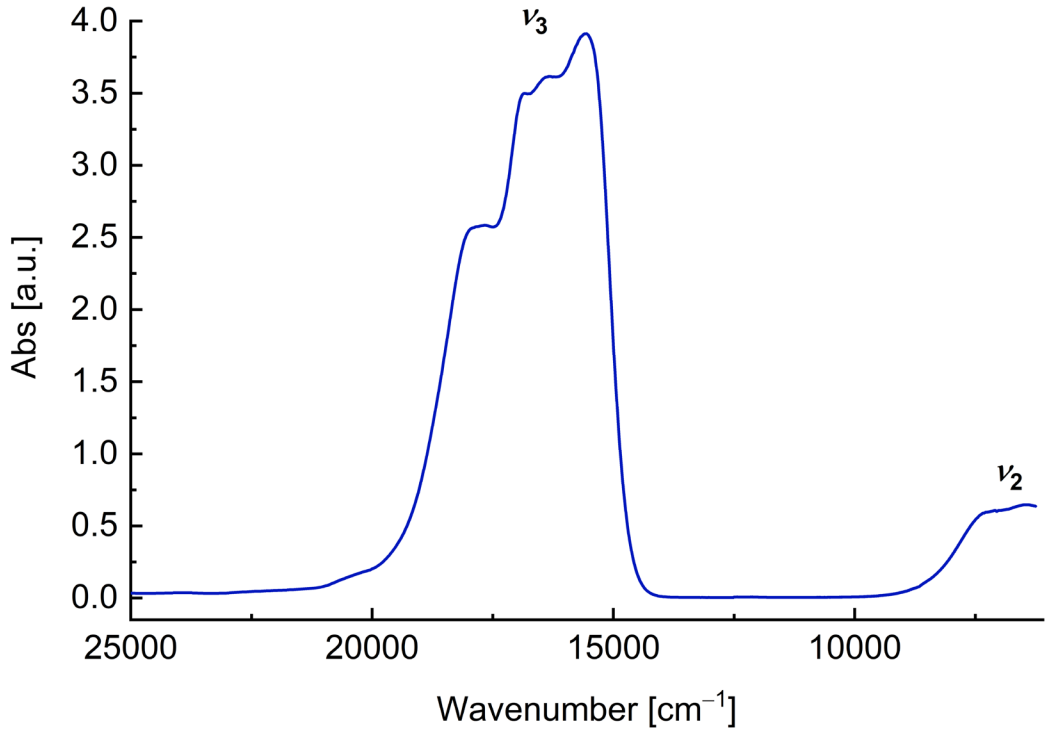

Figure 4. UV-Vis-near-IR spectrum of $[NEt_4]_2[Co(OTeF_5)_4]$ in CH_2Cl_2 (~0.01 M).

2.3. Stability and chemical bonding studies

To get further insights into the nature of $[NEt_4]_2[Co(OTeF_5)_4]$, we studied the stability and the properties of the Co–$OTeF_5$ bond, which had remained elusive until now. In this regard, $[NEt_4]_2[Co(OTeF_5)_4]$ shows a high thermal stability up to 248 °C under strictly inert conditions (see Figure S3), similar to the nickel analogue.[4] Surprisingly, the Co–$OTeF_5$ bonds are stable to ambient conditions, yet under a humid environment, the color of the solid changes from deep blue to pale pink, indicating a change in the coordination geometry from tetrahedral to octahedral,[45] probably due to the coordination of two water molecules (see Supporting Information for additional details). Nevertheless, the teflate ligands likely remain coordinated to the cobalt center, as drying this pink solid under vacuum reverts the process, giving rise to the characteristic deep blue color of the four-coordinate $[NEt_4]_2[Co(OTeF_5)_4]$, as also checked by IR spectroscopy.

One source of information on the character of the Co–$OTeF_5$ bond certainly is the analysis of the IR spectrum of $[NEt_4]_2[Co(OTeF_5)_4]$ (see Figure S1). The Te–O vibration appearing at 834 cm^{-1}, i.e. above 820 cm^{-1}, is indicative of an ionic character of the Co–$OTeF_5$ bond.[46] The similar local coordination environment in the $[CoX_4]^{2-}$ anions (X = $OTeF_5$, F, Cl) prompted us to further investigate the Co–X bonding situation in the $[Co(OTeF_5)_4]^{2-}$ anion and compare it to that of the electronically closely related but hypothetical $[CoF_4]^{2-}$ anion and the known $[CoCl_4]^{2-}$ anion, containing chloride ligands that differ more with respect to the Δ_T they are causing.

For performing theoretical bonding studies we selected the Interacting Quantum Atoms (IQA) energy decomposition scheme.[47] In general terms, this is a chemically meaningful parameter-free and orbital-invariant approach that decomposes the total molecular energy into different

contributions from a scalar topological partition, which in most cases (including this one), is that provided by the quantum theory of atoms-in-molecules (QTAIM) methodology.[48] Namely, the energy is divided into intra-atomic and inter-atomic contributions between pairs of atoms (say A and B). In turn, the inter-atomic contributions can be further decomposed into a classical electrostatic contribution (V_{cl}^{AB}) and an exchange-correlation contribution (V_{xc}^{AB}). The former (V_{cl}^{AB}) is related to the bond ionicity, while the latter (V_{xc}^{AB}) provides a measure of electron delocalization, being directly connected with covalency.[49–51] In fact, the exchange-correlation contribution V_{xc}^{AB} has been recently proposed by Martín Pendás *et al.* to be used as a measure of bond strength, since the electrostatic counterpart (V_{cl}^{AB}) is likely to be affected by long-range interactions, which are specially relevant in systems bearing highly electronegative groups, as it is the case in the ones considered herein.[52] Another significant aspect of the IQA/QTAIM framework is its ability to extend the aforementioned discussion beyond the partitioning of the molecule into individual atoms. Indeed, it can be readily applied to scenarios where the molecule is divided into multiple groups or fragments, each comprised of one or more atoms.[47] In this manner, the teflate group was defined as the collective sum of all the atoms constituting it, and its interaction with cobalt is determined by the summation of pairwise interactions between each of those atoms and the metal center. As we will study the interaction between Co and a given group (X = $OTeF_5$, F or Cl), we will refer to the exchange-correlation interaction terms as V_{xc}^{CoX}.

The strongest bond in terms of V_{xc}^{CoX} corresponds to $[Co(OTeF_5)_4]^{2-}$, being –293.6 kJ mol^{-1}, while the least favorable term, –264.7 kJ mol^{-1}, corresponds to $[CoF_4]^{2-}$ (see Table 1). In the case of the $[CoCl_4]^{2-}$ anion, V_{xc}^{CoX} takes an intermediate value of –277.1 kJ mol^{-1}. It should be noted that the values for the three complexes are relatively similar, indicating a comparable strength of the Co–X bonds in all cases. Additionally, the electronegativity of the X group was studied by

analyzing the QTAIM charge of the Co center. In this regard, the similarity between fluoride and teflate is clear, as both lead to the same charge at the metal center, q(Co) ~1.44 |e$^-$|. As expected, the chloride ligand induces a significantly lower charge at the Co atom, q(Co) = 1.215 |e$^-$|. This result is in line with chlorine having the lowest electronegativity, yet it also reinforces the similarity of the fluoride and teflate ligands in their electron-withdrawing properties.[1,2] Overall, this analysis aligns with the fact that the $[Co(OTeF_5)_4]^{2-}$ anion can be seen as an analogue of $[CoF_4]^{2-}$ in terms of bonding properties, but with the discrete structure of the heavier halogenidocobaltates.

Table 1. Calculated Co–X distance (in pm), V_{xc}^{CoX} (in kJ mol^{-1}) and QTAIM charges (in |e$^-$|) for $[CoX_4]^{2-}$ complexes (X = $OTeF_5$, F, Cl).

X =	d (Co–X)	V_{xc}^{CoX}	q(Co)	q(X)
$OTeF_5$[a]	196.72	–293.6	1.439	–0.860
F	197.62	–264.7	1.443	–0.861
Cl	235.80	–277.1	1.215	–0.804

[a]For structurally distorted $[Co(OTeF_5)_4]^{2-}$ anions, we took average properties, as the values for the four different teflate groups were very similar. Namely, V_{xc}^{CoX} ranged between –293.3 and –293.8 kJ mol^{-1} for the four different ligands.

3. Conclusions

In summary, we have presented a mixed experimental and theoretical study on the $[Co(OTeF_5)_4]^{2-}$ anion, which is the first cobalt pentafluoroorthotellurate complex and constitutes the only group 9 metal teflate species reported thus far. Complex $[NEt_4]_2[Co(OTeF_5)_4]$, whose Co–$OTeF_5$ bonds are stable to ambient conditions, could be prepared through the reaction of $[NEt_4]_2[CoCl_4]$ with $ClOTeF_5$ and exhibits a distorted tetrahedral geometry around the metal center. The electronic structure of the $[Co(OTeF_5)_4]^{2-}$ anion was investigated by means of DFT

and SA-CASSCF/NEVPT2 calculations, showing a pseudo-$^4A_2$ quartet as the ground state ($S = 3/2$). This result is backed experimentally by the determined effective magnetic moment, indicating the presence of three unpaired electrons, as well as by UV/Vis spectroscopy. Our bonding study of the four-coordinate $[CoX_4]^{2-}$ anions (X = $OTeF_5$, F, Cl) through the IQA energy decomposition scheme demonstrates that the strength of the Co–X interaction is similar for the three analogues, being the strongest in case of teflate. In addition, analysis of the charges in the metal center supports the well-known fact that the fluoride and the teflate anions have similar electron-withdrawing properties.

4. Experimental section

4.1. General procedures and materials

All experiments were performed under rigorous exclusion of moisture and oxygen using standard Schlenk techniques. Solids were handled in a MBRAUN UNIlab plus glovebox under an argon atmosphere (O_2 < 0.5 ppm, H_2O < 0.5 ppm). Solvents were dried using a MBraun SPS-800 solvent system (CH_2Cl_2, *n*-pentane), or over 3 Å molecular sieves (*o*-difluorobenzene (*o*DFB)). $[NEt_4]_2[CoCl_4]$[53] and $ClOTeF_5$[16] were prepared as described elsewhere. All other reagents were purchased from standard commercial suppliers and used as received. Elemental analyses (CHNS) were carried out using a VARIO EL elemental analyzer. The IR spectrum shown in Figure S1 was measured on neat solid samples at room temperature inside a glovebox under an argon atmosphere using a Bruker ALPHA FTIR spectrometer with a diamond ATR attachment with 32 scans and a resolution of 4 cm^{-1}. The IR spectrum shown in Figure S4 was recorded on a Nicolet iS50 Advance FTIR by Thermo Fisher Scientific equipped with an ATR unit, with a Ge on KBr beamsplitter and a DLaTGS-KBr detector for MIR and a solid-substrate

beamsplitter with a DLaTGS-PE detector for FI. The electronic spectrum shown in Figure 4 was collected in CH_2Cl_2 solution (~0.01 M) in a Cary5000 UV-Vis-NIR from Agilent between 200 and 1600 nm. Further parameters associated with the measurement were: slit 2 nm, step 1 nm, grating change 800 nm, lamp change 350 nm. Details of the magnetic susceptibility measurements and of the thermogravimetric analysis are given in the Supporting Information.

4.2. Synthesis of $[NEt_4]_2[Co(OTeF_5)_4]$

$[NEt_4]_2[CoCl_4]$ (100 mg, 217 µmol, 1 equiv.) was weighed into a Schlenk flask with a greaseless Teflon stopcock. After cooling down to −196 °C, $ClOTeF_5$ (356 mg, 1.30 mmol, 6 equiv.) was condensed onto it. The mixture was allowed to warm to room temperature under stirring giving rise to the evolution of Cl_2 as a yellow gas. The mixture, which turned first green and immediately afterwards blue, was stirred for 30 minutes. After removal of the volatiles and drying overnight under vacuum, a deep blue solid was obtained and identified as $[NEt_4]_2[Co(OTeF_5)_4]$ (276 mg, 217 µmol, quant.). **IR** (ATR, 298 K, Figure S1): $\tilde{\nu}$ / cm^{-1} = 3001 (w), 1486 (m), 1458 (w), 1443 (w), 1396 (w), 1369 (w), 1186 (w), 1174 (w), 1069 (w), 1053 (w), 1032 (w), 1001 (w), 834 (m, Te–O), 783 (m), 662 (vs, Te–F), 615 (w), 442 (m, Co–O). **Elemental analysis** calcd (%) for $C_{16}H_{40}CoF_{20}N_2O_4Te_4$: C 15.1, H 3.2, N 2.2; found: C 15.5, H 3.1, N 2.3. **UV-Vis** (CH_2Cl_2): λ_{max} / nm = 566, 594, 612, 643, 1364, 1551.

4.3. Crystallography

Blue single crystals suitable for X-ray diffraction were obtained by slow diffusion of a layer of *n*-hexane (1.5 mL) into a solution of $[NEt_4]_2[Co(OTeF_5)_4]$ in *o*DFB (ca. 10 mg in 1.5 mL) at 4 °C. Crystal data were collected with MoKα radiation on a Bruker D8 Venture diffractometer

with a CMOS area detector. Single crystals were picked at –40°C under nitrogen atmosphere and mounted on a 0.15 mm Mitegen micromount using perfluoroether oil. The structures were solved with the ShelXT[54] structure solution program using intrinsic phasing and refined with the ShelXL[55] refinement package using least squares minimizations by using OLEX2.[56] In the structure of $[NEt_4]_2[Co(OTeF_5)_4]$, the F atoms of the $[OTeF_5]^-$ ligand containing O4 are disordered over two positions and were refined with 0.59 and 0.41 partial occupancy each. The program Diamond V4.6.4 was used for visualization.[57] CCDC 2251373 contains the supplementary crystallographic data for this paper. These data are provided free of charge by The Cambridge Crystallographic Data Centre. Crystal data and other details of the structure analyses are summarized in Table S1.

4.4. Computational details

DFT calculations were performed by means of the Gaussian 16 software package.[58] We considered B3LYP[59] (in conjunction with D3BJ dispersion correction scheme[60,61]) and M06L[62] exchange-correlation functionals. For optimizations and transition state search, we applied the Ahlrichs triple-zeta def2-TZVP basis set.[63] The nature of the stationary points was confirmed by analytical frequency analysis.

Multireference calculations on $[Co(OTeF_5)]^{2-}$ were performed on the B3LYP-D3BJ optimized structure by using the ORCA 5.0 package.[64,65] In both, CASSCF and NEVPT2 calculations, we considered the def2-TZVP basis set, as well as the RI approximation to speed up the calculations, in conjunction with def2/JK auxiliary basis set.[66] As stated in the main text, in SA-CASSCF calculations we chose an active space that includes the 3*d* molecular orbitals of the metal, the Co–O orbitals and, to account for the double shell effect, the 4*d* orbitals of Co. This

way, the active space is composed by 14 molecular orbitals and 15 electrons, CAS(15,14), and is shown in Figure S5. In the state average, we included 10 doublets and 10 quartets. Strongly contracted NEVPT2 calculations were performed on top of the SA-CASSCF wavefunction.

IQA calculations were performed on the corresponding monodeterminantal B3LYP-D3BJ/def2-TZVP wavefunctions by using PROMOLDEN CODE.[67] Molecular orbital representations were made by using VESTA software.[68]

ASSOCIATED CONTENT

Supporting Information

IR spectrum of $[NEt_4]_2[Co(OTeF_5)_4]$, crystal data, magnetic susceptibility measurements, thermogravimetric analysis, investigation of the stability to moisture of $[NEt_4]_2[Co(OTeF_5)_4]$, active space molecular orbitals of the $[Co(OTeF_5)_4]^{2-}$ anion, states composition and energy difference, and Cartesian coordinates of the optimized structures (PDF).

AUTHOR INFORMATION

Corresponding Author

*Alberto Pérez-Bitrián. Fachbereich Biologie, Chemie, Pharmazie, Institut für Chemie und Biochemie – Anorganische Chemie, Freie Universität Berlin, Fabeckstraße 34/36, 14195 Berlin (Germany). E-mail: a.perez.bitrian@fu-berlin.de

*Sebastian Riedel. Fachbereich Biologie, Chemie, Pharmazie, Institut für Chemie und Biochemie – Anorganische Chemie, Freie Universität Berlin, Fabeckstraße 34/36, 14195 Berlin (Germany). E-mail: s.riedel@fu-berlin.de

Author Contributions

The manuscript was written through contributions of all authors. All authors have given approval to the final version of the manuscript.

Notes

The authors declare no competing financial interest.

ACKNOWLEDGEMENT

Funded by the Deutsche Forschungsgemeinschaft (DFG, German Research Foundation) – Project-ID 387284271 – SFB 1349 and by the European Research Council (ERC) Project HighPotOx (grant agreement ID: 818862), as well as through the cluster of excellence "UniSysCat" funded by the DFG under Germany's Excellence Strategy-EXC2008/1-390540038. We gratefully acknowledge the assistance of the Core Facility BioSupraMol supported by the DFG. A.P.-B. thanks the Alexander von Humboldt Foundation for a postdoctoral research fellowship, as well as the Department of Biology, Chemistry, Pharmacy of the Freie Universität Berlin for a Rising Star Junior Fellowship. J.M. acknowledges the Spanish MICINN (grant PID2021-122763NBI00) and the FICyT (grant IDI/2021/000054) for financial support, as well as Dr. Carlos Martín-Fernández and Prof. Ángel Martín Pendás for fruitful scientific discussions. The authors thank Dr. Karl David Wegner (Bundesanstalt für Materialforschung und -prüfung) for providing the spectrometer for the measurement of the UV-Vis-near-IR spectrum, and Dr. Thomas Lohmiller (Humboldt-Universität zu Berlin) for the assistance with the fitting of the magnetic data.

REFERENCES

1. Seppelt, K. Stabilization of Unusual Oxidation and Coordination States by the Ligands OSF_5, $OSeF_5$, and $OTeF_5$. *Angew. Chem. Int. Ed. Engl.* **1982**, *21*, 877–888.

2. Gerken, M.; Mercier, H. P. A.; Schrobilgen, G. J. In *Advanced Inorganic Fluorides: Synthesis, Characterization and Applications*; Nakajima, T.; Žemva, B.; Tressaud, A., Eds.; Elsevier Science S.A.: Lausanne, 2000; pp 117–174.

3. Riddlestone, I. M.; Kraft, A.; Schaefer, J.; Krossing, I. Taming the Cationic Beast: Novel Developments in the Synthesis and Application of Weakly Coordinating Anions. *Angew. Chem. Int. Ed.* **2018**, *57*, 13982–14024.

4. Pérez-Bitrián, A.; Hoffmann, K. F.; Krause, K. B.; Thiele, G.; Limberg, C.; Riedel, S. Unravelling the Role of the Pentafluoroorthotellurate Group as a Ligand in Nickel Chemistry. *Chem. Eur. J.* **2022**, *28*, e202202016.

5. Winter, M.; Peshkur, N.; Ellwanger, M. A.; Pérez-Bitrián, A.; Voßnacker, P.; Steinhauer, S.; Riedel, S. Gold Teflates Revisited: from the Lewis Superacid $[Au(OTeF_5)_3]$ to the Anion $[Au(OTeF_5)_4]^-$. *Chem. Eur. J.* **2023**, *29*, e202203634.

6. Alvarez, S.; Cirera, J. How High the Spin? Allowed and Forbidden Spin States in Transition-Metal Chemistry. *Angew. Chem. Int. Ed.* **2006**, *45*, 3012–3020.

7. Davidson, P. J.; Lappert, M. F.; Pearce, R. Stable Homoleptic Metal Alkyls. *Acc. Chem. Res.* **1974**, *7*, 209–217.

8. Fernández-Valparís, J.; Alvarez, S. Design of a structural database for homoleptic transition metal complexes. *Struct. Chem.* **2015**, *26*, 1715–1723.

9. Schröder, K.; Sladky, F. Darstellung und Eigenschaften von $TiCl_{4-n}(OTeF_5)_n$(n = 1–4), $Cs_2[Ti(OTeF_5)_6]$ und $Ti(OTeF_5)_4 \cdot 2POCl_3$. *Chem. Ber.* **1980**, *113*, 1414–1419.

10. Van Seggen, D. M.; Hurlburt, P. K.; Anderson, O. P.; Strauss, S. H. Weakly Coordinating Anions $M(OTeF_5)_6^-$ (M = Nb, Sb) and $M(OTeF_5)_6^{2-}$ (M = Ti, Zr, Hf): Two-Step Synthesis, Characterization, Stability, and Use in the Isolation of the Dihaloalkane Complex Cations $Ag(CH_2Cl_2)_3^+$, $Ag(CH_2Br_2)_3^+$, and *catena*-poly[$Ag(1,2\text{-}C_2H_4Br_2)_2$-$\mu$-(1,2-$C_2H_4Br_2$)-*Br*:*Br'*]$^+$. *Inorg. Chem.* **1995**, *34*, 3453–3464.

11. Seppelt, K. Übergangsmetall-pentafluoroorthochalcogenate. *Chem. Ber.* **1975**, *108*, 1823–1829.

12. Drews, T.; Seppelt, K. $Fe(OTeF_5)_3$, Darstellung, Struktur und Reaktivität. *Z. Anorg. Allg. Chem.* **1991**, *606*, 201–207.

13. Blackman, A. G. Cobalt: Inorganic & Coordination Chemistry. In *Encyclopedia of Inorganic Chemistry*, 2nd ed.; King, R. B., Ed.; Wiley: Chichester, 2006.

14. Strauss, S. H. The Search for Larger and More Weakly Coordinating Anions. *Chem. Rev.* **1993**, *93*, 927–942.

15. Seppelt, K.; Nothe, D. Stability of Xenon(II) Compounds. The Pentafluorooxyselenium and Pentafluorooxytellurium Radicals. Bis(pentafluorotellurium) Peroxide and Chlorine Pentafluoroorthotellurate. *Inorg. Chem.* **1973**, *12*, 2727–2730.

16. Schack, C. J.; Christe, K. O. New syntheses of pentafluorotellurium hypochlorite. *J. Fluorine Chem.* **1982**, *21*, 393–396.

17. Lentz, D.; Seppelt, K. $OTeF_5$-Verbindungen von P, As und Sb. *Z. Anorg. Allg. Chem.* **1983**, *502*, 83–88.

18. Turowsky, L.; Seppelt, K. Rheniumverbindungen mit dem Liganden -$OTeF_5$. *Z. Anorg. Allg. Chem.* **1990**, *590*, 37–47.

19. Turowsky, L.; Seppelt, K. Molybdän- und Wolframverbindungen mit dem Liganden -$OTeF_5$. *Z. Anorg. Allg. Chem.* **1990**, *590*, 23–36.

20. Vij, A.; Wilson, W. W.; Vij, V.; Corley, R. C.; Tham, F. S.; Gerken, M.; Haiges, R.; Schneider, S.; Schroer, T.; Wagner, R. I. Methyl Tin(IV) Derivatives of $HOTeF_5$ and $HN(SO_2CF_3)_2$: A Solution Multinuclear NMR Study and the X-ray Crystal Structures of $(CH_3)_2SnCl(OTeF_5)$ and $[(CH_3)_3Sn(H_2O)_2][N(SO_2CF_3)_2]$. *Inorg. Chem.* **2004**, *43*, 3189–3199.

21. Seppelt, K. Neue Derivate der Pentafluoroorthoselensäure, Halogenderivate der Pentafluoroorthotellursäure. *Chem. Ber.* **1973**, *106*, 1920–1926.

22. Zadrozny, J. M.; Telser, J.; Long, J. R. Slow magnetic relaxation in the tetrahedral cobalt(II) complexes $[Co(EPh)_4]^{2-}$ (E=O, S, Se). *Polyhedron* **2013**, *64*, 209–217.

23. Elinburg, J. K.; Doerrer, L. H. Synthesis, structure, and electronic properties of late first-row transition metal complexes of fluorinated alkoxides and aryloxides. *Polyhedron* **2020**, *190*, 114765.

24. Cantalupo, S. A.; Lum, J. S.; Buzzeo, M. C.; Moore, C.; DiPasquale, A. G.; Rheingold, A. L.; Doerrer, L. H. Three-coordinate late transition metal fluorinated alkoxide complexes. *Dalton Trans.* **2010**, *39*, 374–383.

25. Buzzeo, M. C.; Iqbal, A. H.; Long, C. M.; Millar, D.; Patel, S.; Pellow, M. A.; Saddoughi, S. A.; Smenton, A. L.; Turner, J. F. C.; Wadhawan, J. D.; Compton, R. G.; Golen, J. A.; Rheingold, A. L.; Doerrer, L. H. Homoleptic Cobalt and Copper Phenolate $A_2[M(OAr)_4]$ Compounds: The Effect of Phenoxide Fluorination. *Inorg. Chem.* **2004**, *43*, 7709–7725.

26. Petersen, M. V.; Iqbal, A. H.; Zakharov, L. N.; Rheingold, A. L.; Doerrer, L. H. Fluorinated phenolates in monomeric and dimeric Co(II) compounds. *Polyhedron* **2013**, *52*, 276–283.

27. Yang, L.; Powell, D. R.; Houser, R. P. Structural variation in copper(I) complexes with pyridylmethylamide ligands: structural analysis with a new four-coordinate geometry index, τ_4. *Dalton Trans.* **2007**, 955–964.

28. Figgis, B. N.; Lewis, J. The Magnetic Properties of Transition Metal Complexes. *Prog. Inorg. Chem.* **1964**, *6*, 37–239.

29. Figgis, B. N. Magnetic Properties of Spin-Free Transition Series Complexes. *Nature* **1958**, *182*, 1568–1570.

30. Cotton, F. A.; Goodgame, D. M. L.; Goodgame, M. The Electronic Structures of Tetrahedral Cobalt(II) Complexes. *J. Am. Chem. Soc.* **1961**, *83*, 4690–4699.

31. Cotton, F. A.; Goodgame, M. Magnetic Investigations of Spin-free Cobaltous Complexes. V. Tetra-azido and Tetracyanato Cobaltate(II) Ions. *J. Am. Chem. Soc.* **1961**, *83*, 1777–1780.

32. Roos, B. O.; Taylor, P. R.; Sigbahn, P. E. M. A complete active space SCF method (CASSCF) using a density matrix formulated super-CI approach. *Chem. Phys.* **1980**, *48*, 157–173.

33. Angeli, C.; Cimiraglia, R.; Evangelisti, S.; Leininger, T.; Malrieu, J.-P. Introduction of *n*-electron valence states for multireference perturbation theory. *J. Chem. Phys.* **2001**, *114*, 10252–10264.

34. Angeli, C.; Cimiraglia, R.; Malrieu, J.-P. *N*-electron valence state perturbation theory: a fast implementation of the strongly contracted variant. *Chem. Phys. Lett.* **2001**, *350*, 297–305.

35. Angeli, C.; Cimiraglia, R.; Malrieu, J.-P. *n*-electron valence state perturbation theory: A spinless formulation and an efficient implementation of the strongly contracted and of the partially contracted variants. *J. Chem. Phys.* **2002**, *117*, 9138–9153.

36. Pierloot, K.; Phung, Q. M.; Domingo, A. Spin State Energetics in First-Row Transition Metal Complexes: Contribution of (3s3p) Correlation and Its Description by Second-Order Perturbation Theory. *J. Chem. Theory Comput.* **2017**, *13*, 537–553.

37. Pierloot, K. Transition metals compounds: Outstanding challenges for multiconfigurational methods. *Int. J. Quantum Chem.* **2011**, *111*, 3291–3301.

38. Boguslawski, K.; Marti, K. H.; Legeza, Ö.; Reiher, M. Accurate *ab Initio* Spin Densities. *J. Chem. Theory Comput.* **2012**, *8*, 1970–1982.

39. Haupt, A. In *Organic and Inorganic Fluorine Chemistry*; de Gruyter: Berlin/Boston, 2021; pp 235–245.

40. Welsch, M.; Babel, D. Kristallstruktur-Verfeinerungen an Rubidiumtetrafluorometallaten(II): Rb_2MF_4 (M = Mg, Co, Ni). *Z. Naturforsch. B* **1991**, *46*, 161–164.

41. Keve, E. T.; Abrahams, S. C.; Bernstein, J. L. Ferroelectric Paraelastic Paramagnetic Barium Cobalt Fluoride, $BaCoF_4$, Crystal Structure. *J. Chem. Phys.* **1970**, *53*, 3279–3287.

42. Babel, D.; Herdtweck, E. Abstands- und Koordinations-Verhältnisse in den Schichtstrukturen der ternären Fluoride K_2MF_4 und $K_3M_2F_7$(M^{II} = Mg, Mn, Co–Zn). *Z. Anorg. Allg. Chem.* **1982**, *487*, 75–84.

43. Wiesner, J. R.; Srivastava, R. C.; Kennard, C. H. L.; Di Vaira, M.; Lingafelter, E. C. The Crystal Structures of Tetramethylammonium Tetrachloro-cobaltate(II), -nickelate(II), and -zincate(II). *Acta Cryst*. **1967**, *23*, 565–574.

44. Lever, A. B. P. In *Inorganic Electronic Spectroscopy*; Elsevier: New York, 1984; pp. 479–506.

45. Cotton, F. A.; Wilkinson, G.; Murillo, C. A.; Bochmann, M. In *Advanced Inorganic Chemistry*, 6th ed.; Wiley: New York, 1999; pp 814–835.

46. Strauss, S. H.; Noirot, M. D.; Anderson, O. P. Preparation and Characterization of Silver(I) Teflate Complexes: Bridging $OTeF_5$ Groups in the Solid State and in Solution. *Inorg. Chem.* **1985**, *24*, 4307–4311.

47. Blanco, M. A.; Martín Pendás, A.; Francisco, E. Interacting Quantum Atoms: A Correlated Energy Decomposition Scheme Based on the Quantum Theory of Atoms in Molecules. *J. Chem. Theory Comput.* **2005**, *1*, 1096–1109.

48. Bader, R. F. W. *Atoms in Molecules - A Quantum Theory*. Clarendon Press: Oxford, 1994.

49. Guevara-Vela, J. M.; Francisco, E.; Rocha-Rinza, T.; Martín Pendás, Á. Interacting Quantum Atoms—A Review. *Molecules*, **2020**, *25*, 4028.

50. Francisco, E.; Menéndez Crespo, D.; Costales, A.; Martín Pendás, Á. A Multipolar Approach to the Interatomic Covalent Interaction Energy. *J. Comput. Chem.* **2017**, *38*, 816–829.

51. Martín Pendás, Á.; Francisco, E.; Suárez, D.; Costales, A.; Díaz, N.; Munárriz, J.; Rocha-Rinza, T.; Guevara-Vela, J. M. Atoms in molecules in real space: a fertile field for chemical bonding. *Phys. Chem. Chem. Phys.* **2023**, *25*, 10231–10262.

52. Martín Pendás, A.; Casals-Sainz, J. L.; Francisco, E. On Electrostatics, Covalency, and Chemical Dashes: Physical Interactions versus Chemical Bonds. *Chem. Eur. J.* **2019**, *25*, 309–314.

53. Gill, N. S.; Taylor, F. B.; Hatfield, W. E.; Parker, W. E.; Fountain, C. S.; Bunger, F. L. In *Inorganic Syntheses, Volume IX*; Tyree, S. Y., Jr., Ed.; McGraw-Hill Book Co.: New York, 1967; pp 136–142.

54. Sheldrick, G. M. Structure determination revisited. *Acta Cryst. A* **2015**, *71*, s9.

55. Sheldrick, G. M. Crystal structure refinement with *SHELXL*. *Acta Cryst. C* **2015**, *71*, 3–8.

56. Dolomanov, O. V.; Bourhis, L. J.; Gildea, R. J.; Howard, J. A. K.; Puschmann, H. *OLEX2*: a complete structure solution, refinement and analysis program. *J. Appl. Cryst.* **2009**, *42*, 339–341.

57. Brandenburg, K. *DIAMOND*, Crystal Impact GbR: Bonn, 2014.

58. Frisch, M. J.; Trucks, G. W.; Schlegel, H. B.; Scuseria, G. E.; Robb, M. A.; Cheeseman, J. R.; Scalmani, G.; Barone, V.; Petersson, G. A.; Nakatsuji, H.; Li, X.; Caricato, M.; Marenich, A. V.; Bloino, J.; Janesko, B. G.; Gomperts, R.; Mennucci, B.; Hratchian, H. P.; Ortiz, J. V.; Izmaylov, A. F.; Sonnenberg, J. L.; Williams-Young, D.; Ding, F.; Lipparini, F.; Egidi, F.; Goings, J.; Peng, B.; Petrone, A.; Henderson, T.; Ranasinghe, D.; Zakrzewski, V. G.; Gao, J.; Rega, N.; Zheng, G.; Liang, W.; Hada, M.; Ehara, M.; Toyota, K.; Fukuda, R.; Hasegawa, J.; Ishida, M.; Nakajima, T.; Honda, Y.; Kitao, O.; Nakai, H.; Vreven, T.; Throssell, K.; Montgomery, J. A., Jr.; Peralta, J. E.; Ogliaro, F.; Bearpark, M. J.; Heyd, J. J.; Brothers, E. N.; Kudin, K. N.; Staroverov, V. N.; Keith, T. A.; Kobayashi, R.; Normand, J.; Raghavachari, K.; Rendell, A. P.; Burant, J. C.; Iyengar, S. S.; Tomasi, J.; Cossi, M.; Millam, J. M.; Klene, M.; Adamo, C.; Cammi, R.; Ochterski, J. W.; Martin, R. L.; Morokuma, K.; Farkas, O.; Foresman, J. B.; Fox, D. J. *Gaussian 16 (Revision C.01)*, Gaussian, Inc.: Wallingford, CT, 2016.

59. Becke, A. D. A new mixing of Hartree-Fock and local-density-functional theories. *J. Chem. Phys.* **1993**, *98*, 1372–1377.

60. Grimme, S.; Antony, J.; Ehrlich, S.; Krieg, H. A consistent and accurate *ab initio* parametrization of density functional dispersion correction (DFT-D) for the 94 elements H-Pu. *J. Chem. Phys.* **2010**, *132*, 154104.

61. Johnson, E. R.; Becke, A. D. A post-Hartree–Fock model of intermolecular interactions. *J. Chem. Phys.* **2005**, *123*, 024101.

62. Zhao, Y.; Truhlar, D. G. A new local density functional for main-group thermochemistry, transition metal bonding, thermochemical kinetics, and noncovalent interactions. *J. Chem. Phys.* **2006**, *125*, 194101.

63. Weigend, F.; Ahlrichs, R. Balanced basis sets of split valence, triple zeta valence and quadruple zeta valence quality for H to Rn: Design and assessment of accuracy. *Phys. Chem. Chem. Phys.* **2005**, *7*, 3297–3305.

64. Neese, F. Software update: The ORCA program system—Version 5.0. *WIREs Comput. Mol. Sci.* **2022**, *12*, e1606.

65. Neese, F. The ORCA program system. *WIREs Comput. Mol. Sci.* **2012**, *2*, 73–78.

66. Weigend, F. Hartree-Fock Exchange Fitting Basis Sets for H to Rn. *J. Comput. Chem.* **2008**, *29*, 167–175.

67. Martín Pendás, A.; Francisco, E. *Promolden: A QTAIM/IQA code* (available from the authors upon request).

68. Momma, K.; Izumi, F. *VESTA 3* for three-dimensional visualization of crystal, volumetric and morphology data. *J. Appl. Cryst.* **2011**, *44*, 1272–1276.

For Table of Contents Only

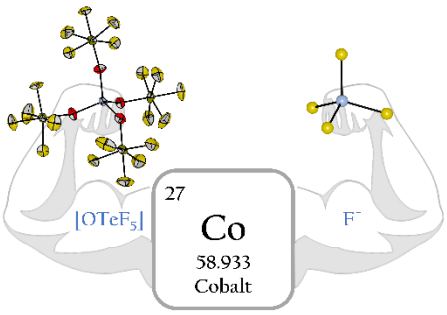

The $[Co(OTeF_5)_4]^{2-}$ anion is the first group 9 metal teflate complex to be prepared and characterized. Through this combined experimental and theoretical study, the $[OTeF_5]^-/F^-$ analogy in coordination chemistry is further supported.